

Ab initio prediction of a two-dimensional variant of the iridate IrO_2

Andriy Smolyanyuk,¹ Markus Aichhorn,¹ I.I. Mazin,² and Lilia Boeri^{3,4}

¹*Institute of Theoretical and Computational Physics, Graz University of Technology, NAWI Graz, 8010 Graz, Austria*

²*Code 6393, Naval Research Laboratory, Washington, DC 20375, USA*

³*Department of Physics, Sapienza Università di Roma, 00185 Rome, Italy*

⁴*Istituto dei Sistemi Complessi (ISC)-CNR, 00185 Rome, Italy*

(Dated: June 16, 2022)

We propose a novel insulating 2D phase of IrO_2 , predicted by *ab initio* evolutionary algorithms. The predicted phase is a van der Waals crystal, in which Ir forms a triangular lattice, and is energetically competitive with the metastable spinel phase, observed experimentally. Electronic structure calculations show that the magnetic properties of this phase are highly nontrivial, with an almost perfect degeneracy of 120° Neel and Y-stripe orders, and unusually soft magnetic moments. The resulting behavior, which we term *easy plane anisotropy*, is entirely different from what is realized in previously-explored Kitaev honeycomb lattices. Our results thus suggest that IrO_2 may be an ideal candidate to realize highly unusual magnetic properties.

PACS numbers: 71.20.Be, 71.30.+h, 73.61.Ng, 73.90.+f, 75.70.Ak

I. INTRODUCTION

Two-dimensional materials represent an ideal platform to investigate exotic physical phenomena, such as charge-density wave, superconductivity, topological order, etc., and have a wide range of applicability in different fields, ranging from coating to 2D electronics.¹⁻³ The best known systems are usually obtained by mechanical exfoliation of bulk van der Waals crystals, such as graphene⁴ (graphite), *h*-BN,⁵ transition metal dicalcogenides (TMDC),⁶ or MXenes.⁷

Besides investigating the properties of materials derived from known bulk phases, an emerging trend in the field of 2D materials is to use computational methods in order to discover, predict and characterize completely new structures. For example, Ref. 8 investigated the stability of single-layer MX_2 transition-metal oxides and dichalcogenides in honeycomb-like structures, data mining of structures listed in various databases was employed to filter out possible 2D materials,⁹ high-throughput computations were used to determine possible exfoliation of experimentally known compounds,¹⁰ and evolutionary algorithms were used to predict new 2D materials.^{11,12}

Most 2D materials known up to now are non-magnetic metals, semiconductors or insulators. The Mermin-Wagner theorem postulates that magnetic order is forbidden in the two-dimensional Heisenberg model at finite temperature.¹³ However, recently magnetism in 2D van der Waals crystals was discovered,^{14,15} showing that long-range magnetic order is indeed possible in 2D systems, since magnetic anisotropy removes the restriction coming from the Mermin-Wagner theorem. This opens the road to the discovery of many other 2D magnetic systems.

In this work, using evolutionary crystal structure prediction, we identify a novel 2D phase of IrO_2 , which may be the first realization of a purely 2D system with strongly anisotropic magnetic interactions, including, but not limited to, the Kitaev interaction. The Ki-

taev model¹⁶ has been studied theoretically by several authors.¹⁷⁻¹⁹ Experimental realizations have been proposed in several systems, such as, for instance, Na_2IrO_3 , $\alpha\text{-Li}_2\text{IrO}_3$, Li_2RhO_3 and $\alpha\text{-RuCl}_3$.²⁰ The first proposal by Jackeli *et al.*²¹ was to realize the Kitaev model on the triangular lattice formed by edge-shared IrO_6 octahedra, typical, for instance, in layered ABO_2 compounds where *A* and *B* are alkali and transition metal ions, respectively. In all the above proposals, the transition metal sublattice is effectively embedded in a three-dimensional framework, while in 2D- IrO_2 the Kitaev physics may be realized even on a single monolayer.

Using first-principles calculations based on Density Functional Theory (DFT), we find that our new 2D- IrO_2 structure is dynamically stable, van der Waals bound (*i.e.*, easy to exfoliate), and most intriguingly, exhibits a highly unusual discrete magnetic frustration, namely, a 120° noncollinear structure with a particular spin orientation with respect to crystallographic axes is essentially degenerate with a stripe order, again with a specific spin orientation. This degeneracy cannot be reproduced by a short-range bilinear coupling, whether isotropic or anisotropic, and may have ramifications far beyond the scope of this paper.

Even more unusual is the softness of the Ir magnetic moment, which can only have a full magnetization consistent with $j_{\text{eff}} = 1/2$ when the moments lie in the plane. If rotated away from the plane, the moment rapidly collapses to essentially zero. This is in some sense similar to the popular XY model, but this similarity is misleading: in the XY model magnetic moments are strictly restricted within the plane, while in our case they can be rotated away, but their amplitude rapidly decreases with the angle; such excitations, impossible in the XY model, are allowed here, so that the system would have different spin dynamics, different response to magnetic field, and even different thermodynamics. Such systems have never been studied before and represent a new intriguing class of magnetic models.

Our paper is structured as follows: in Section II we introduce the 1T-IrO₂ structure, and study its energetics and structural stability; in Section III we describe the effect of crystal field, spin-orbit coupling and local electronic correlations on the electronic structure; in the next section, IV, we discuss the unusual magnetic properties predicted by DFT, and the relevance of different model Hamiltonians to our results. Finally, in the Appendix we describe the details of the evolutionary search that led us to discover 2D-IrO₂, and provide the computational details used for all our calculations.

II. CRYSTAL STRUCTURE AND STRUCTURAL STABILITY

The crystal structure of 2D-IrO₂ is shown in Fig. 1; it is analogous to the 1T-polytype of many TMDC. In this structure, iridium is arranged on a triangular lattice, at the centers of O₆ octahedra, with slight trigonal distortion (negative). The space group of the structure is $P\bar{3}2/m1$; the lattice parameters are: $a=b=3.16$ Å, $\alpha=\beta=90^\circ$, $\gamma=120^\circ$ and sufficiently large vacuum layer was inserted. The Ir atom is situated at Wyckoff position (1a) (0,0,0), while O is situated at Wyckoff position (2d) ($\frac{1}{3}, \frac{2}{3}, 0.073$).

Our 1T-IrO₂ structure, as detailed in the Appendix, was identified almost accidentally through a sequence of several evolutionary crystal structure runs, and appears to be a very stable local minimum of the energy landscape of IrO₂, where the dominant minima are the two known bulk phases, with rutile²² and spinel²³ structures. To

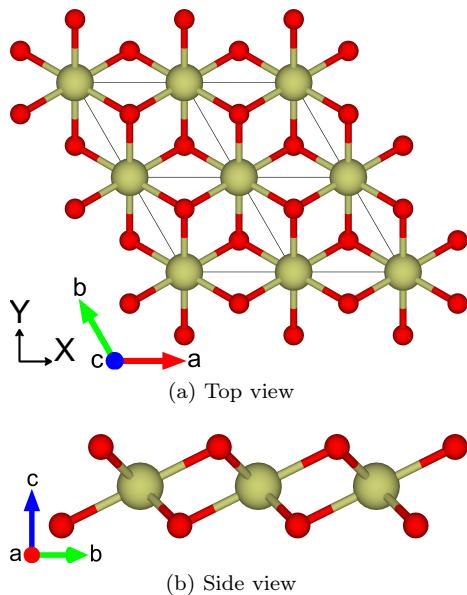


Figure 1. (Color online) 1T-IrO₂ polytype crystal structure: dark-gray (red) are oxygen atoms, light-gray (green) are iridium atoms; (a) top view, (b) side view. The X, Y axes indicate the global (XYZ) coordinate system

Table I. Comparison of energies of various 2D IrO₂ phases (nonmagnetic calculations including SOC).

Name	Energy/Atom (meV)
Rutile (bulk)	0
1T	237
Spinel (bulk)	266
Rutile (001)	326
Rutile (110)	385
1H	621

the best of our knowledge, this is the first time that a 2D structure is predicted for IrO₂; however, 2D structures that are markedly different from the bulk structures have been predicted for other binary oxides, such as SiO₂ and TiO₂.^{24,25}

Table I lists the energetics of different IrO₂ phases. The stabilization energy of 1T-IrO₂ (~ 240 meV/atom) compared to the bulk rutile phase, is in the same ballpark as what is found for many compounds that exhibit competing layered and bulk phases, such as diamond and graphite,²⁶ h - and cubic BN,²⁷ etc. Indeed, 1T-IrO₂ appears to be not only more stable energetically than other 2D polytypes,²⁸ but also compared to surface terminations of the rutile ground-state structure and to the first metastable bulk phase, *i.e.* spinel; thus, it could be very likely synthesized experimentally.

According to our calculation, 1T-IrO₂ is stable in both monolayer and bulk form; in fact, our calculations suggest that the latter becomes the ground state at ~ 160 GPa, overcoming the two 3D bulk structures. This bulk layered phase is a van der Waals crystal, as can be demonstrated by optimizing with and one without a van der Waals correction (we used the one from Ref. 29, but it is well-known that alternative choices yield similar results). We found that the interlayer distance in the two cases differs by 3.3 Å (9.65 vs. 6.35 Å), which is larger than for representative transition metal dichalcogenides (7.4 – 6.0 = 1.4 Å for MoS₂, 6.9 – 6.0 = 0.9 Å for NbSe₂), and similar to that in graphite (8.8 – 6.6 = 2.2 Å).³⁰ This means that, once synthesized, 1T-IrO₂ will be easily exfoliable.

After the structure was determined, we checked its dynamical stability by calculating the phonon dispersion. We used a finite displacement method as implemented in the Phonopy package,³¹ using a 2x2x1 supercell. Under realistic conditions, *i.e.*, including SOC, strong correlations and magnetism (see next paragraph), 1T-IrO₂ is dynamically stable.

III. ELECTRONIC STRUCTURE

Ir⁴⁺ has one unpaired electron, residing in the $j_{\text{eff}} = 1/2$ state, so one expects the ground state to be magnetic. As commonly done for Ir⁴⁺ compounds, we have included

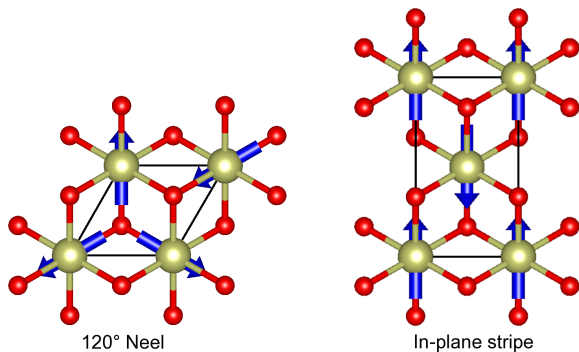


Figure 2. (Color online) The two nearly-degenerate 1T-IrO₂ magnetic configurations, which are lowest in energy. The arrows show the directions of the spin magnetic moments on the Ir atoms in the XY plane.

electronic correlations using the GGA+U method with $U - J = 2$ eV, a typical value for such systems.³²⁻³⁴ Our calculations show no qualitative changes in the properties of 1T-IrO₂ for $1.3 < U - J < 4.0$ eV.

We find two completely different magnetic ground states, degenerate on the level of computational accuracy of $\lesssim 1$ meV/Ir. These two configurations are the 120°-Neel orientation and an *inplane stripe* order with magnetic moments directed along the global Y axis, which we will denote as *Y-stripes*, as shown in Fig. 2. The 120°-Neel configuration is formed by three sublattices oriented at a 120° angle with respect to each other, and the Y-stripes configuration is formed by antiferromagnetically coupled rows of collinear spins lying in the layer's plane.

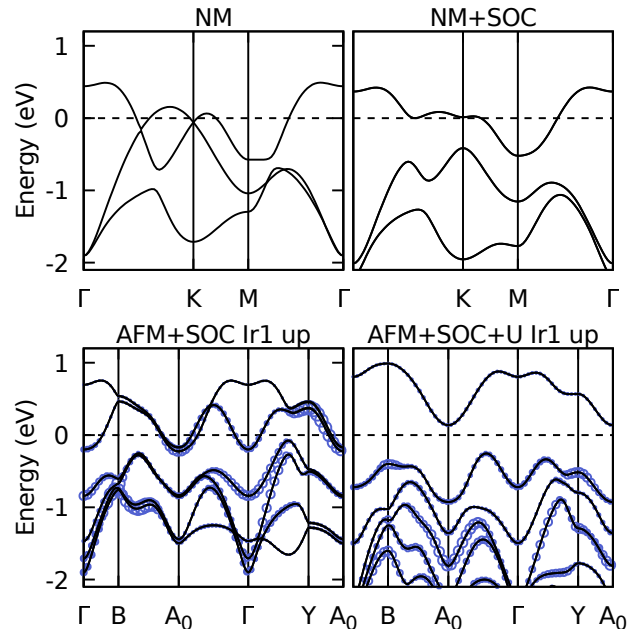
In both cases the system forms a weak Mott-Hubbard insulator; using $U - J = 2.0$ eV, the band gap for the 120°-Neel structure is 0.42 eV and for the Y-stripes it is 0.24 eV.

The origin of the gap is the same as in other Ir⁴⁺ iridates. The t_{2g} splits into a $j_{\text{eff}} = 1/2$ doublet and a $j_{\text{eff}} = 3/2$ quartet. The former forms a narrow half-filled band that can be easily split by a moderate Hubbard interaction.³⁶ As one can see in the lower panel of Fig. 3, already for $U = 0$ the exchange splitting is trying to open the gap, but it is too weak. Adding a finite U eventually opens up a gap.

IV. MAGNETIC STRUCTURE

Magnetic interactions are strongly anisotropic (see Table II and top panel of Fig. 4). For rotations of the stripe order out of the XY-plane the minimum of the energy corresponds to the in-plane direction, while for rotations in the XY-plane the Y direction, orthogonal to an Ir-Ir bond, is energetically more favorable. Importantly, as Fig. 4 shows, as magnetic moments are rotated away from the XY plane by more than approximately 15°, they collapse from 0.4-0.5 μ_B to 0.1 μ_B or less (numbers are given for spin moments; the total moments drop from about 1.0

Figure 3. Band structure of 1T-IrO₂ states for nonmagnetic IrO₂ with and without spin-orbit coupling (top panel), and the Y-stripe AFM configuration with SOC and with or without $U = 2.7$ eV. Calculations are done with Wien2k.³⁵ The bottom panels show the projection on the single Ir spin-up states. The high-symmetry k -points are: (upper panel) $\Gamma(0, 0, 0)$, $K(\frac{1}{3}, \frac{1}{3}, 0)$, $M(\frac{1}{2}, 0, 0)$ for trigonal cell ($a=b=3.16$ Å, $\alpha=\beta=90^\circ$, $\gamma=120^\circ$) and (bottom panel) $\Gamma(0, 0, 0)$, $B = (\frac{1}{2}, 0, 0)$, $Y = (0, \frac{1}{2}, 0)$, $A_0 = (\frac{1}{2}, \frac{1}{2}, 0)$ for monoclinic supercell ($a=3.16$ Å, $b=5.47$ Å, $\alpha = \beta = \gamma = 90^\circ$).



to 0.2-0.25 μ_B).

It has become customary to use the anisotropic exchange model, sometimes called Heisenberg-Kitaev Hamiltonian, for describing magnetic interactions in iridates. It can be conveniently written using the form suggested in Ref. 18, 21, and 37:

$$\begin{aligned}
 H = & \sum_{\langle ij \rangle} J (S_i^x S_j^x + S_i^y S_j^y + \Delta S_i^z S_j^z) \\
 & + 2J_{\pm\pm} ((S_i^x S_j^x - S_i^y S_j^y)c_\alpha - (S_i^x S_j^y + S_i^y S_j^x)s_\alpha) \\
 & + J_{z\pm} ((S_i^y S_j^z + S_i^z S_j^y)c_\alpha - (S_i^x S_j^z + S_i^z S_j^x)s_\alpha),
 \end{aligned} \tag{1}$$

In the notations of Ref. 21, $J_{\pm\pm} = \frac{1}{6}(2\Gamma' - 2\Gamma - K)$, $J_{z\pm} = \frac{\sqrt{2}}{3}(K - \Gamma + \Gamma')$, $J\Delta = \frac{1}{3}(3J + K + 2\Gamma + 4\Gamma')$. While the easy-plane anisotropy is not affected by pure Kitaev interactions, it is affected by the non-Kitaev terms Γ and Γ' . The sum above is over the nearest-neighboring sites i and j ; $c_\alpha = \cos \varphi_\alpha$ and $s_\alpha = \sin \varphi_\alpha$, where $\varphi_\alpha = \{0, \frac{2\pi}{3}, -\frac{2\pi}{3}\}$ is the bond angle between the direction of the ij bond and the X axis. J is the bond-independent isotropic magnetic interaction term, $J_{\pm\pm}$ and $J_{z\pm}$ are the bond-dependent anisotropic terms and Δ is what is usually called Ising exchange; $\Delta < 0$ corresponds to an easy Z-axis, and $\Delta > 0$ to an XY easy-plane anisotropy.

The easy-plane anisotropy that we see in the calculations, is, on the first glance, an indication of a sizeable $\Delta > 0$. However, a closer look reveals that in our case the most important contribution to the anisotropy does not come from Δ , but from the magnetic moment softening for out-of-plane directions (see the bottom panel of Fig. 4). This strong softening of the magnetic moment makes it impossible to use a fully 3D model Hamiltonian with rigid magnetic moments, such as the Heisenberg-Kitaev model, to describe the magnetic interactions. It is, on the other hand, possible to describe magnetic interactions for spins restricted to the XY plane, using a 2D-restricted version of this model, namely

$$H = \sum_{\langle ij \rangle} J (S_i^x S_j^x + S_i^y S_j^y) + 2J_{\pm\pm} ((S_i^x S_j^x - S_i^y S_j^y)c_\alpha - (S_i^x S_j^y + S_i^y S_j^x)s_\alpha). \quad (2)$$

The classical per-site energies of the phases with magnetization directions in the XY plane, namely the 120° order, rotations of the stripe order in the XY plane and an in-plane FM order (see Fig. 4 and Table II) are

$$E_{120} = E_0 - \frac{3}{2}J, \quad (3)$$

$$E_{XY}^{Stripe} = E_0 - J - 4J_{\pm\pm} \cos 2\theta, \quad (4)$$

$$E_{FM} = E_0 + 3J, \quad (5)$$

where $\theta = 0$ corresponds to the Y -direction.

The least-squares fit of J , $J_{\pm\pm}$ and E_0 to the available data is shown in Table III, while the energies predicted by the fitted model for different magnetic configurations are shown in the last column of Table II (E_{fit}). The agreement in this case is quite good, indicating that the in-plane restricted model is a rather good match for DFT energies.

The anisotropic $J_{\pm\pm}$ term is only three times smaller than the isotropic J term, emphasizing strong *in-plane* anisotropy. This is in addition to the above-mentioned nontrivial anisotropy stemming from the softness of magnetic moments. The degeneracy of the 120° Neel and the Y -stripe configurations is only reproduced within 4 meV, while in the calculations the two configurations are degenerate within a fraction of meV. Such an accidental discontinuous degeneracy, a consequence of the intrinsic magnetic frustration, adds a further exciting aspect to the unusual spin dynamics of this system.

V. CONCLUSIONS

We predicted a novel insulating layered phase of IrO_2 with a triangular Ir^{4+} lattice – 1T- IrO_2 . We show that it is likely to be a very stable, albeit not the most stable phase. The bonding between the layers is very weak, so monolayers could be easily obtained by exfoliation. The Ir^{4+} ions are in an (approximately) $j_{\text{eff}} = 1/2$ state, as

Table II. Energy and absolute values of the spin and orbital magnetic moments for different magnetic phases. The direction of the magnetic moment is denoted in the global coordinate system; the last column shows energies (per formula unit) estimated using the in-plane Hamiltonian Eq. (2) with the parameters from Table III. Note that the energy fits are not applicable to out-of-plane directions, lines 3 and 7.

Name	Energy/f.u. (meV)	m_s (μ_B)	m_l (μ_B)	E_{fit} (meV)
120 Neel	0	0.40	0.50	4
Y-stripe	0	0.43	0.55	0
Z-stripe	9	0.09	0.11	-
X-stripe	16	0.35	0.50	16
Y-FM	34	0.47	0.61	35
X-FM	34	0.47	0.61	35
Z-FM	49	0.09	0.16	-

Table III. Parameters of the restricted Heisenberg-Kitaev Hamiltonian Eq. (2), obtained by a least-square fit.

J (meV)	$J_{\pm\pm}$ (meV)	E_0 (meV)
6.7 ± 0.4	2.0 ± 0.2	14.4 ± 0.5

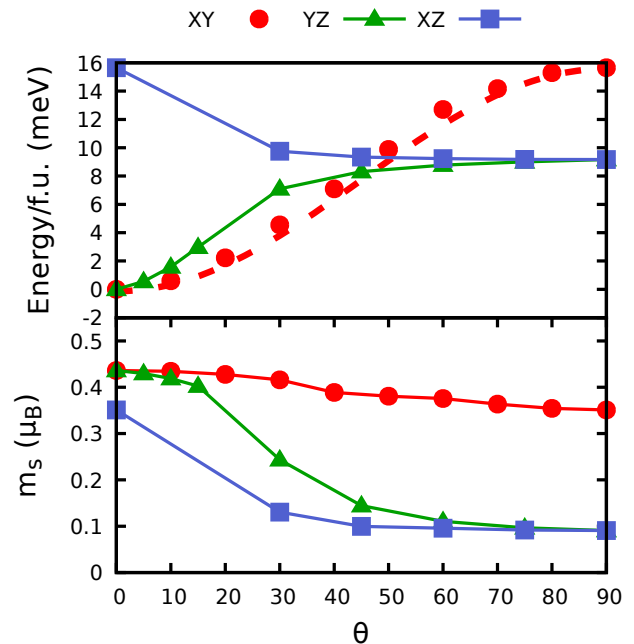


Figure 4. Dependence of the energy (top panel) and the spin magnetic moment on the Ir site (bottom panel) on the rotation angle for stripe order, with spins rotating in the XY (circles), YZ (triangles) and XZ (squares) planes. The dashed line is the fit of energy of XY rotations to the model defined by Eq. (2). For rotations in the XY plane, θ is the in-plane rotation angle, and $\theta = 0$ corresponds to the Y direction; for rotations in the YZ and XZ planes, the angle θ is the out-of-plane rotation angle, with $\theta = 0$ indicating the in-plane direction. Solid lines are meant as a guide to the eye.

are most other Ir⁴⁺ iridates, too. Our *ab initio* calculations reveal several highly unusual aspects of magnetism in this system: (i) a nontrivial accidental degeneracy of the magnetic ground state: the 120° Neel orientation and the *Y*-stripe (in-plane orientation perpendicular to the Ir-Ir bonds) are degenerate down to 1 meV/atom; (ii) a strong magnetic anisotropy even within the hexagonal plane, a reflection of strong bond-dependent magnetic exchange interactions; (iii) finally, the calculated moments are exceptionally soft in the sense that they essentially disappear if forced to tilt away from the plane. This behavior can be called an “easy plane anisotropy”, but this anisotropy is physically very distinct from the “conventional” easy plane behavior, provided by either single-site or exchange anisotropy. Thus, despite the same geometry as honeycomb iridates, in 1T-IrO₂ Kitaev interaction does not strongly dominate the magnetic physics. This system is entirely different from previously explored Kitaev honeycomb lattices, and promises new and nontrivial magnetic properties.

ACKNOWLEDGMENTS

We acknowledge funding from the Austrian Science Fund FWF through SFB ViCoM, Project F04115 and START program Y746, and computational resources from the VSC3 of the Vienna University of Technology and HPC TU Graz. I.I. Mazin acknowledges support by ONR through the NRL basic research program and Sapienza University of Rome through Bando Professori Visitatori 2018.

APPENDIX: COMPUTATIONAL DETAILS

Details of the crystal structure search

Our new structure was identified through a sequence of several evolutionary crystal structure runs, performed with the USPEX package^{38–40} employing four-step structural relaxation. First, in an unbiased 3D structure search, we realized that metastable 2D structures of IrO₂, with stabilization energies of 200 meV, coexisted with the known bulk structures. For a further refinement we repeated the search with different accuracies, but limiting our search to 2D structures. This yielded 1T as the most stable polytype,²⁸ also compared to (001) and (110) cuts of the rutile surface, see Table I.

Details of DFT calculation

To calculate the total energies and perform structural optimization we used density functional theory (DFT) in the generalized gradient approximation (GGA) with Perdew-Burke-Ernzerhof functional^{41,42} as implemented in the VASP package^{43–46} using the projector augmented wave method (PAW).^{47,48}

For the post-processing of the results from the evolutionary search and calculation of properties the energy cutoff was set to 600 eV, and a Γ -centered Monkhorst-Pack grid^{49,50} with the reciprocal-space resolution of $0.023 \text{ 2}\pi \text{ \AA}^{-1}$ was used. For the magnetic calculations the Wigner-Seitz radius was set to 1.423 \AA and 0.9 \AA for Ir and O atoms respectively; the penalty term λ for constrained magnetic calculations was set to the value 10.

The band structure plots shown in Fig. 3 were obtained with Wien2k.⁵¹ Due to different implementations of the GGA+U method in VASP and Wien2k, the value of U is not directly transferable between the two codes. For that reason, we had to use a slightly larger value of $U = 2.7 \text{ eV}$ when using Wien2k. This value yields a similar gap as for VASP calculations with $U = 2.0 \text{ eV}$. For the Wien2k calculations we used a 16x16x1 k-mesh, defined on Γ -centered point grid.⁵²

¹ K. S. Novoselov, A. Mishchenko, A. Carvalho, and A. H. C. Neto, *Science* **353**, aac9439 (2016).

² J. Wang, F. Ma, and M. Sun, *RSC Advances* **7**, 16801 (2017).

³ G. Fiori, F. Bonaccorso, G. Iannaccone, T. Palacios, D. Neumaier, A. Seabaugh, S. K. Banerjee, and L. Colombo, *Nature Nanotechnology* **9**, 768 (2014).

⁴ K. S. Novoselov, A. K. Geim, S. V. Morozov, D. Jiang, Y. Zhang, S. V. Dubonos, I. V. Grigorieva, and A. A. Firsov, *Science* **306**, 666 (2004).

⁵ A. Nagashima, N. Tejima, Y. Gamou, T. Kawai, and C. Oshima, *Phys. Rev. Lett.* **75**, 3918 (1995).

⁶ M. Bosi, *RSC Advances* **5**, 75500 (2015).

⁷ M. Khazaei, A. Ranjbar, M. Arai, T. Sasaki, and S. Yunoki, *Journal of Materials Chemistry C* **5**, 2488 (2017).

⁸ C. Ataca, H. Şahin, and S. Ciraci, *The Journal of Physical Chemistry C* **116**, 8983 (2012).

⁹ S. Lebègue, T. Björkman, M. Klintonberg, R. M. Nieminen, and O. Eriksson, *Physical Review X* **3** (2013), 10.1103/PhysRevX.3.031002.

¹⁰ N. Mounet, M. Gibertini, P. Schwaller, D. Campi, A. Merkys, A. Marrazzo, T. Sohier, I. E. Castelli, A. Cepellotti, G. Pizzi, and N. Marzari, *Nature Nanotechnology*

- 13**, 246 (2018).
- ¹¹ A. R. Oganov, J. Chen, C. Gatti, Y. Ma, Y. Ma, C. W. Glass, Z. Liu, T. Yu, O. O. Kurakevych, and V. L. Solozhenko, *Nature* **457**, 863 (2009).
 - ¹² X.-F. Zhou, X. Dong, A. R. Oganov, Q. Zhu, Y. Tian, and H.-T. Wang, *Physical Review Letters* **112** (2014), 10.1103/PhysRevLett.112.085502.
 - ¹³ N. D. Mermin and H. Wagner, *Physical Review Letters* **17**, 1133 (1966).
 - ¹⁴ B. Huang, G. Clark, E. Navarro-Moratalla, D. R. Klein, R. Cheng, K. L. Seyler, D. Zhong, E. Schmidgall, M. A. McGuire, D. H. Cobden, W. Yao, D. Xiao, P. Jarillo-Herrero, and X. Xu, *Nature* **546**, 270 (2017).
 - ¹⁵ C. Gong, L. Li, Z. Li, H. Ji, A. Stern, Y. Xia, T. Cao, W. Bao, C. Wang, Y. Wang, Z. Q. Qiu, R. J. Cava, S. G. Louie, J. Xia, and X. Zhang, *Nature* **546**, 265 (2017).
 - ¹⁶ A. Kitaev, *Annals of Physics* **321**, 2 (2006), January Special Issue.
 - ¹⁷ I. Kimchi and A. Vishwanath, *Physical Review B* **89**, 014414 (2014).
 - ¹⁸ J. Chaloupka and G. Khaliullin, *Physical Review B* **92**, 024413 (2015).
 - ¹⁹ J. Chaloupka and G. Khaliullin, *Physical Review B* **94**, 064435 (2016).
 - ²⁰ S. M. Winter, A. A. Tsirlin, M. Daghofer, J. van den Brink, Y. Singh, P. Gegenwart, and R. Valentí, *Journal of Physics: Condensed Matter* **29**, 493002 (2017).
 - ²¹ G. Jackeli and G. Khaliullin, *Physical Review Letters* **102** (2009), 10.1103/PhysRevLett.102.017205.
 - ²² V. Goldschmidt, T. Barth, G. Lunde, and W. Zachariasen, *Skrifter utgitt av det Norske Videnskaps-Akademi i Oslo 1: Matematisk-Naturvidenskapelig Klasse* (1926) , 1 (1926).
 - ²³ H. Kuriyama, J. Matsuno, S. Niitaka, M. Uchida, D. Hashizume, A. Nakao, K. Sugimoto, H. Ohsumi, M. Takata, and H. Takagi, *Applied Physics Letters* **96**, 182103 (2010).
 - ²⁴ V. O. Özçelik, S. Cahangirov, and S. Ciraci, *Physical Review Letters* **112** (2014), 10.1103/PhysRevLett.112.246803.
 - ²⁵ H. A. Eivari, S. A. Ghasemi, H. Tahmasbi, S. Rostami, S. Faraji, R. Rasoulkhani, S. Goedecker, and M. Amsler, *Chemistry of Materials* **29**, 8594 (2017).
 - ²⁶ H. Shin, S. Kang, J. Koo, H. Lee, J. Kim, and Y. Kwon, *The Journal of Chemical Physics* **140**, 114702 (2014), <https://doi.org/10.1063/1.4867544>.
 - ²⁷ A. Janotti, S.-H. Wei, and D. J. Singh, *Phys. Rev. B* **64**, 174107 (2001).
 - ²⁸ A. Guinier (Chairman), G. B. Bokij, K. Boll-Dornberger, J. M. Cowley, S. Đurovič, H. Jagodzinski, P. Krishna, P. M. de Wolff, B. B. Zvyagin, D. E. Cox, P. Goodman, T. Hahn, K. Kuchitsu, and S. C. Abrahams, *Acta Crystallographica Section A* **40**, 399 (1984).
 - ²⁹ A. Tkatchenko and M. Scheffler, *Phys. Rev. Lett.* **102**, 073005 (2009).
 - ³⁰ T. Bučko, S. Lebègue, J. Hafner, and J. G. Ángyán, *Phys. Rev. B* **87**, 064110 (2013).
 - ³¹ A. Togo and I. Tanaka, *Scripta Materialia* **108**, 1 (2015).
 - ³² S. M. Winter, Y. Li, H. O. Jeschke, and R. Valentí, *Phys. Rev. B* **93**, 214431 (2016).
 - ³³ P. Liu, S. Khmelevskiy, B. Kim, M. Marsman, D. Li, X.-Q. Chen, D. D. Sarma, G. Kresse, and C. Franchini, *Phys. Rev. B* **92**, 054428 (2015).
 - ³⁴ K. Li, S.-L. Yu, and J.-X. Li, *New Journal of Physics* **17**, 043032 (2015).
 - ³⁵ The value of U was set to 2.7 eV (0.2 Ry) since higher U is needed to open the gap when calculations are employed by `Wien2k` due to the difference between implementations (value of U is not transferable between `VASP` and `Wienk2` software).
 - ³⁶ B. J. Kim, H. Jin, S. J. Moon, J.-Y. Kim, B.-G. Park, C. S. Leem, J. Yu, T. W. Noh, C. Kim, S.-J. Oh, J.-H. Park, V. Durairaj, G. Cao, and E. Rotenberg, *Phys. Rev. Lett.* **101**, 076402 (2008).
 - ³⁷ P. A. Maksimov, Z. Zhu, S. R. White, and A. L. Chernyshev, *Phys. Rev. X* **9**, 021017 (2019).
 - ³⁸ A. R. Oganov and C. W. Glass, *The Journal of Chemical Physics* **124**, 244704 (2006), 10.1063/1.2210932.
 - ³⁹ A. O. Lyakhov, A. R. Oganov, H. T. Stokes, and Q. Zhu, *Computer Physics Communications* **184**, 1172 (2013).
 - ⁴⁰ A. R. Oganov, A. O. Lyakhov, and M. Valle, *Accounts of Chemical Research* **44**, 227 (2011).
 - ⁴¹ J. P. Perdew, K. Burke, and M. Ernzerhof, *Phys. Rev. Lett.* **77**, 3865 (1996).
 - ⁴² J. P. Perdew, K. Burke, and M. Ernzerhof, *Phys. Rev. Lett.* **78**, 1396 (1997).
 - ⁴³ G. Kresse and J. Hafner, *Phys. Rev. B* **47**, 558 (1993).
 - ⁴⁴ G. Kresse and J. Hafner, *Phys. Rev. B* **49**, 14251 (1994).
 - ⁴⁵ G. Kresse and J. Furthmüller, *Computational Materials Science* **6**, 15 (1996).
 - ⁴⁶ G. Kresse and J. Furthmüller, *Phys. Rev. B* **54**, 11169 (1996).
 - ⁴⁷ G. Kresse and D. Joubert, *Phys. Rev. B* **59**, 1758 (1999).
 - ⁴⁸ P. E. Blöchl, *Phys. Rev. B* **50**, 17953 (1994).
 - ⁴⁹ H. J. Monkhorst and J. D. Pack, *Phys. Rev. B* **13**, 5188 (1976).
 - ⁵⁰ J. D. Pack and H. J. Monkhorst, *Phys. Rev. B* **16**, 1748 (1977).
 - ⁵¹ P. Blaha, K. Schwarz, G. K. H. Madsen, D. Kvasnicka, and J. Luitz, *WIEN2K, An Augmented Plane Wave + Local Orbitals Program for Calculating Crystal Properties* (Karlheinz Schwarz, Techn. Universität Wien, Austria, 2001).
 - ⁵² P. E. Blöchl, O. Jepsen, and O. K. Andersen, *Phys. Rev. B* **49**, 16223 (1994).